Food Chemistry: X 17 (2023) 100570

Contents lists available at ScienceDirect

Food Chemistry: X

journal homepage: www.sciencedirect.com/journal/food-chemistry-x

Comparison of chemical property and in vitro digestion behavior of polysaccharides from *Auricularia polytricha* mycelium and fruit body

Zhengbin Yang [a,c,d], Yongde Zeng [b], Yuedan Hu [a,c,d], Tingting Zhou [a,c,d], Jiamin Li [a,c,d], Lapin He [a,c,d], Wei Zhang [e], Xuefeng Zeng [a,b,c,d,*], Jin Fan [a,c,d,*]

[a] School of Liquor and Food Engineering, Guizhou University, Guiyang, China
[b] Guizhou Industrial Technology Research Institute of Rare Edible and Medicinal Fungi Co., Ltd, Guiyang 550025, China
[c] Guizhou Provincial Key Laboratory of Agricultural and Animal Products Storage and Processing, Guiyang, China
[d] Key Laboratory of Animal Genetics, Breeding and Reproduction in the Plateau Mountainous Region, Ministry of Education, Guiyang, China
[e] College of Food Science and Engineering, Wuhan Polytechnic University, Wuhan, China

ARTICLE INFO

Keywords:
Auricularia polytricha
Fruit body
Mycelium
Polysaccharides
In vitro digestion

ABSTRACT

The antioxidant activity of *Auricularia polytricha* is associated tightly with its polysaccharide concentration, molar mass and architecture. This study aims to explore the differences in structural and physicochemical traits and oxidation resistances between the polysaccharides from fruit body (ABPs) and mycelial (IAPs) of *Auricularia polytricha*. The results showed that ABPs and IAPs were constituted by glucose, glucuronic acid, galactose and mannose. However, the molecular weight distribution of IAPs (3.22×10^4 Da (52.73%) and 1.95×10^6 Da (24.71%)) was wider than that of ABPs (5.4×10^6 Da (95.77%)). The shear-thinning performance and viscoelastic behavior of both IAPs and ABPs are representative. IAPs are scattered in sheets, with folds and holes, and have a triple helix structure. ABPs are compact in structure and clear in texture. The main functional groups and thermal stability of both polysaccharides were similar. Concerning the in-vitro oxidation resistance, both of the studied polysaccharides exhibited the potent potential to scavenge hydroxyl radicals ($IC_{50} = 3.37 \pm 0.32$ and 6.56 ± 0.54 mg/mL, respectively) and 1,1-diphenyl-2-picrylhydrazyl (DPPH) radicals ($IC_{50} = 0.89 \pm 0.22$ and 1.48 ± 0.63 mg/mL, respectively), as well as the moderate reduction power. In addition, IAPs and ABPs were both completely undigested in simulated contexts of saliva, small intestine and stomach, and the two polysaccharide types maintained high DPPH and hydroxyl radical scavenging activities. DDPH scavenging rate during digestion was positively correlated with uronic acid content. To conclude, this study suggests the potential of IAPs as an equivalent alternative to ABPs.

Introduction

Auricularia polytricha-10 is an edible mushroom of *Auriculariaceae* and a common industrialized variety in the edible fungus industry, whose yearly production is approximately 1,000,000 t. *Auricularia polytricha* is a very popular ingredient in Chinese traditional cuisine and is deeply loved by a large population. Therefore, it has a broad market in China. It has a long history as an edible and medicinal mushroom in East Asia, including China (Sheu, Chien, Chien, Chen, & Chin, 2004). It has high carbohydrate and protein contents and diverse physiological properties, such as anti-tumor, antioxidant and immune regulation activities (Chen & Xue, 2018; Sangphech, Sillapachaiyaporn, Nilkhet, & Chuchawankul, 2021; Yu, Sun, Zhao, & Wang, 2014; Zhao et al., 2015). Being a healthy food with good antioxidant function, its fruit body has been widely used mainly due to its rich polysaccharides. Biofunctions of polysaccharides are associated with their composition, Mw, branching degree and sulfonation degree (Ma, Chen, Zhu, & Wang, 2013), besides, the contents of phenols and proteins in polysaccharides and their complexation degree will affect their antioxidant activities. The molecular weight of polysaccharide exerts a significant impact on its biological activity, and the antioxidant effect of low molecular weight polysaccharide is better than that of high molecular weight polysaccharide (Sun, Wang, & Zhou, 2012).

Currently, research concerning the polysaccharides from *Auricularia polytricha* emphasizes the biological actions and macromolecular structural traits of polysaccharides in fruit body (Chen et al., 2018, Zhang

* Corresponding authors at: School of Liquor and Food Engineering, Guizhou University, Guiyang, China.
E-mail addresses: heiniuzxf@163.com (X. Zeng), 529715291@qq.com (J. Fan).

https://doi.org/10.1016/j.fochx.2023.100570
Received 6 October 2022; Received in revised form 16 December 2022; Accepted 6 January 2023
Available online 7 January 2023

et al., 2020). Nevertheless, due to the disadvantages of high cultivation cost, low yield and high risk, fruiting bodies often cause soil, atmosphere and water pollutions to varying degrees to the growing environment of edible fungi, which can be ascribed to the discharge of industrial wastes and the extensive use of chemical pesticides, directly or indirectly causing excessive toxicity of edible fungi and high content of harmful substances. It has been reported that upon severe contamination of cultivation matrix, the maximum absorption of Pb in *Auricularia auricula*, *Lentinus edodes* and *Pleurotus ostreatus* can be up to 150–200 mg/kg. With a maximum cumulant of 180 mg/kg, *Lentinus edodes* exhibits a more prominent cumulative effect on Cd (Lei & Yang, 1990). Moreover, considering the seasonality constraint and scant land resources, the naturally grown agaric has been unable to satisfy the current demand, and its industrialization has thus been restricted. One strategy to overcome these problems is to grow the mycelium of *Auricularia polytricha* in liquid media (submerged fermentation), whose superiorities include short duration of cultivation, small space occupation, cost efficiency, as well as ease of stimulant supplementation to increase the cultivation yield (Xiao et al., 2020). Fermentation mycelium is considered as a potential alternative to natural fruiting bodies. Because polysaccharides are hydrophilic macromolecules with complex structure, diverse components and large molecular weight, their alterations in the digestive system of humans are yet to be clarified thoroughly. Determination of polysaccharide changes during gastrointestinal digestion is of great significance for evaluating potential bioactivities of compounds and establishing bioaccessibility. Based on the research reports, thorough degradation and absorption of polysaccharides are hardly achievable in the digestive system of humans. In an in-vitro simulated digestive context, thorough degradation of polysaccharides from Fuzhuan brick tea (Chen et al., 2018) and *Lycium barbarum* (Ding et al., 2019) was found to be impossible, which directly reached the large intestine. Intestinal microflora functions crucially in secretase decomposition of polysaccharides, and in the insubstantial generation of short-chain fatty acids (SCFAs). Currently, there is no systematic evaluation of the difference between mycelial and fruit body polysaccharides of *Auricularia polytricha* and whether they can be decomposed in the alimentary system (saliva, stomach and small intestine), whether there is any change in antioxidant activity during digestion, and what is the difference between them.

In the early stage, the process was optimized by fermenting *Auriculariapolytricha*'s yellow slurry water, and subsequently precipitating and separating the polysaccharides (APP40, APP60 and APP80) by gradient concentration of ethanol (40%, 60% and 80%). The yielded 3 crude polysaccharides were examined for physicochemical traits, oxidation resistance sand primary structures via SEM, XRD, FT-IR, AFM and other instruments. It lays the foundation for this study (Yang et al., 2022). Accordingly, this study attempts to compare the differences between mycelial and fruit polysaccharides in a systematical manner, mainly including the following four parts: (1) Physicochemical properties (total carbohydrate, total protein, uronic acid, etc.). (2) Differences in composition and molecular weight distribution of monosaccharides. (3) By comparing the structural properties (functional groups, morphology, triple helix structure, thermodynamic properties, etc.) of mycelium polysaccharides and fruit body polysaccharides, the similarities between them were pointed out. (4) Furthermore, the antioxidant activity changes of mycelial polysaccharide and fruit body polysaccharide during digestion were investigated by simulating human saliva-gastrointestinal digestion model in vitro.

Materials and methods

Materials and reagents

Strain and fruit body of *Auricularia polytricha*-10 were procured from Tianda Institute of Edible Fungi (Jiangdu, Jiangsu, China) and Chengdu Edible Fungus Base (Sicuan, China), respectively. Standard monosaccharides, including arabinose, mannose, lyxose, glucose, rhamnose, xylose and galactose, were purchased from Lanji Technology Development (Shanghai). The rest reagents and chemicals were all analytically pure.

Submerged cultivation and preparation of A. polytricha polysaccharides

Submerged cultivation was also employed to acquire the mycelia. Initially, 10 pieces of *A. polytricha* mycelia were transferred into an Erlenmeyer flask (250 mL) that contained the liquid fermentation medium (100 mL, potato extract (20%), glucose (2%), KH_2PO_4 (0.2%) and $MgSO_4{\cdot}7H_2O$ (0.1%), pH: natural) for overnight standing. Following 4-day incubation of the culture on a rotary shaker under 170 rpm and 26 ℃ conditions, the Erlenmeyer flasks (5 L) filled with liquid fermentation medium (3 L) were added with liquid seeds (10% inoculum volume). Thereafter, the flasks were incubated for a 3-day period on a rotary shaker under 170 rpm and 26 ℃, and the fermentation medium was discarded. After twice washing in distilled water, the filter residue was lyophilized to obtain dried mycelia. The fruit body was washed, dried, pulverized and sieved via a sieve (100 mesh) to decolorize and remove small molecular substances. First, the samples (15.0 g) were refluxed for a 2-h period twice using 80% (v/v) ethanol (150 mL) at 80 ℃. Then, the remaining residue was centrifuged and placed in the oven at 60 ℃, dried and sealed for storage. The extraction of polysaccharides from *A. polytricha* is as follows:

Ultrasonically assisted extraction was accomplished through a slightly modified version of the optimized method (Fu et al., 2020).The prepared mycelium and fruit body 5 g were extracted with 200 mL deionized water by Cell Crusher 450 W for 20 min. After centrifugation (8000 rpm, 10 min), the extracts mixed with trypsin (250:1, v:m) was used to remove protein at 40 ℃ for 20 min. After the reaction, the added enzyme was inactivated by heating (90 ℃). The solution was centrifuged to remove the precipitation (8000 rpm, 10 min). The extracts were subject to overnight precipitation at 4 ℃ using 4 volumes of 95% (v/v) ethanol. The solution was later centrifuged to remove the supernatant, the polysaccharide precipitate was fully dissolved with distilled water, and finally the remaining ethanol solution was concentrated and removed. The lyophilized powdery polysaccharides from *A. polytricha* mycelia were referred to as the intracellular polysaccharides (IAPs), while the polysaccharide from fruiting bodies were referred to as ABPs.

Molecular properties of IAPs and ABPs

Chemical composition

Total polysaccharide concentrations of IAPs and ABPs were estimated by the phenol–sulfuric acid approach (Dubois, Gilles, Hamilton, Rebers, & Smith, 1956). Bradford's method was utilized to assess the protein concentrations of these two polysaccharide types, where bovine serum albumin was used as the standard (Bradford, 1976). M-hydroxydiphenyl method was employed to measure the uronic acid levels in IAPs and ABPs, where the used standard was galacturonic acid (Filisetti-Cozzi & Carpita, 1991). The reducing sugar concentrations were examined by the dinitrosalicylic acid method (Miller, 1959).

Determination of molecular weights

Through High Performance Gel Filtration Chromatography (HPGFC), the Molecular Weights (Mw) estimation of polysaccharide fractions was accomplished using a HPLC system (2414 refractive index detector and 1525pump, Waters, USA), where a size exclusion Linear 300 mm × 7.8 mmid × 2 column (Ultrahydrogel) was installed. The mobile phase was sodium nitrate (0.1 M), the column temperature was 45 ℃, and the flow rate was 0.9 mL/min. The sample was prepared by dissolving in the mobile phase and filtering through the micropore membrane (0.45 μm). The chromatographic diagram of molecular weight calibration curve is shown in Fig. 1S. The molecular weight calibration curves were adopted by the following standards:

MW135350, MW36800, MW9750, MW2700 and MW180, and the corresponding retention times were 15.08 min, 15.50 min, 18.25 min, 18.98 min and 21.47 min, respectively. Linear regression equation: y = -0.4851x + 12.758 (R^2 = 0.9965).

Determination of constituent monosaccharides

Polysaccharide sample (5 mg) was dispensed in a plugged calibration tube (20 mL), added with 1 mL of TFA (2 M), and subjected to a 2 h hydrolysis under a 121 ℃ condition in an oven. After making the volume to 50 mL with water, the samples were filtered with the micropore membrane (0.45 μm) for subsequent injection analysis. Through High Performance Anion Exchange Chromatography (HPAEC), the monosaccharides were compositionally elucidated using an ICS-5000 (Dionex) equipped with a 3 mm × 150 mm TMPA20 column (CarboPac). NaOH (250 mM) was used to elute the column at 0.5 mL/min, while a pulsed amperometric detector was utilized for surveillance of the monosaccharides. The chromatographic diagram of the mixed standard sample is shown in Fig. 2S.

Characterization of IAPs and ABPs

Rheological measurements analysis

ARES-G2- Rotary rheometer (ARES-G2, TA instruments, New Castle, USA) was utilized to estimate the apparent viscosities of IAPs and ABPs at the concentrations of 0.5 % and 1 % (w/v), where a 1.0-mm-gap parallel steel plate (diameter: 5 cm) was utilized. Under 25℃, the flow curve determination of IAPs and ABPs was accomplished at shear rates between 0.01 and 100 s^{-1}. A parallel steel plate was utilized to assess the dynamic oscillation of the two polysaccharides. Initially, the linear viscoelastic zone was identified for every sample by the strain sweep at a 1-Hzfixed oscillation frequency. Then, the storage modulus (Gsticew Castle BPs instruments two polysaccharides were separately estimated within the linear viscoelastic zone through oscillation frequency sweep of 1–100 rad/s under the condition of 25 ℃.

Fourier transform infrared spectroscopy (FTIR) analysis

A FTIR spectrometer (Frontier, PerkinElmer, Boston, USA) was utilized to assess the FTIR spectra of the freeze-dried ABPs and IAPs. Using Spectrum 10.4.2.279 (Frontier, PerkinElmer, Boston, USA), the entire spectra were obtained within the frequency scope of 4,000–500 cm^{-1} (wave number) through the attenuated total reflectance. The measurement of the entire samples was triplicated.

SEM analysis

Sticky carbon tape (double-side) was utilized to evenly adhere the dried IAPs and ABPs to the sample stage. Then, gold powder was used to coat these polysaccharides. A secondary-electron SEM system (1,000–20,000× magnification; SU8010, HITACHI, Japan) was utilized to conduct the examination, which was operated in high vacuum mode at a high voltage of 10.0 kV.

Congo red analysis

IAPs and ABPs were subjected to Congo red detection as per the prior procedure and briefly modified (Rozi et al., 2020). In brief, we mixed 1 mg/mL sample solution (1 mL) with 100 μM Congo red (1 mL) and 1 M sodium hydroxide (varying volumes), followed by the addition of distilled water, aiming to make the final concentration range of sodium hydroxide be 0–0.5 M. After 3 min of preservation at room temperature, the wavelength of maximum absorption (λ_{max}) was documented over a 400–700 nm range with Spectra maxM5, Molecular Devices, USA.

X-ray diffraction (XRD) analysis

Empyrean X-ray diffractometer (PANalytical B.V., Netherlands) was utilized to obtain the XRD data of the two polysaccharides under 45-kV voltage and a 40-mA current. The sweeping scope of diffraction intensities on the powder was 5–80°(2θ angle range), where the step size was 0.013°and the counting time was 0.1 s/step (Tang et al., 2021).

Thermal stability

A STA449C thermogravimetric analyzer (Netzsch, Germany) was adopted for evaluating the polysaccharide samples via thermogravimetry (TG), derivative thermogravimetry (DTG), as well as differential scanning calorimetry (DSC), where the used reference was an empty aluminum crucible. The measurement was approximately 15 mg with the temperature of 25 ℃ to 600 ℃ at 10 ℃ /min under N_2 atmosphere (Tenore, Campiglia, Giannetti, & Novellino, 2015).

In vitro saliva-gastrointestinal digestion

Simulated saliva digestion of IAPs and ABPs

A slightly revised version of reported approach (Tenore et al., 2015) was applied to perform the simulated saliva digestion. Initially, we mixed 5 mg/mL IAPs or ABPs solution (10 mL) with simulated saliva medium (10 mL) comprising NaCl (175.3 g/L), $NaHCO_3$ (84.7 g/L), KCl (89.6 g/L), KSCN (20.0 g/L), NaH_2PO_4 (88.8 g/L), Na_2SO_4 (57.0 g/L), urea (2.0 g/L) and α-amylase (290 mg). Subsequently, 0.1 M HCl was used to make the pH of mixture to 6.8. Under a 37 ℃ condition, the mixture was incubated by steam bath oscillation. Each 2.0 mL of digested samples was collected separately at 0.25 h, 0.5 h and 1 h for further analysis, which were subjected to 5 min boiling to deactivate α-amylase. Digestions were all triplicated. After centrifugation, it was stored at 4 ℃ for use.

Stimulated gastric digestion

A slightly revised version of reported approach (Chen et al., 2018) was applied to explore the simulated gastric digestion. Initially, we mixed 5 mg/mL IAPs or ABPs solution (10 mL) with stimulated gastric medium (10 mL, pH 3) including KCl (1.1 g/L), NaCl (3.1 g/L), $CaCl_2{\cdot}2H_2O$ (0.15 g/L), $NaHCO_3$ (0.6 g/L), 1 M CH_3COONa(10 mL, pH 5), Na_2SO_4 (57.0 g/L), urea (2.0 g/L), gastric pepsin (35.4 mg) and gastric lipase (37.5 mg). Under 37 ℃, the mixture was incubated by steam bath oscillation. Each 2.0 mL of digested samples was collected separately at 0.5 h, 1 h, 2 h, 4 h and 6 h of digestion, and was instantly immersed for 5 min into a boiling water to deactivate enzymes. Digestions were all triplicated. After centrifugation, it was placed at 4 ℃ for use.

Simulated small intestinal digestion

Exploration of simulated small intestinal digestion was accomplished as per a reported approach (Zhou et al., 2018). Initially, we mixed the digestive gastric digestive fluid with the simulated small intestine medium (NaCl (5.4 g/L), KCl (0.65 g/L), $CaCl_2{\cdot}2H_2O$ (0.33 g/L), 1.75 % (w/w) pancreatin,1% (w/w) bile salt and 0.065 mg/g trypsin) at a 10:3. Then, a simulated small intestinal digestion was performed in accordance with the above description. Under 37 ℃, the mixture was incubated by steam bath oscillation. Each 2.0 mL of digested samples was collected separately at 0.5 h, 1 h, 2 h, 4 h and 6 h of digestion, and was instantly immersed for 5 min into a boiling water to deactivate enzymes. Digestions were all triplicated. After centrifugation, it was stored at 4 ℃ for use.

Determination of the antioxidant activity

DPPH radical scavenging activity

The DPPH eliminating activities were evaluated for IAPs and ABPs as per a somewhat revised version of prior procedure (Zhao et al., 2019). Initially, 100 μL of DPPH solution (0.2 mM in ethanol) was added into 100 different concentration IAPs, ABPs solution. A Spectra maxM5 microplate reader (Molecular Devices, USA) was utilized to estimate the 517 nm absorbance following 30 min of interaction in the dark at room temperature, where the positive control was BHT. The computational equation for DPPH scavenging activity was as shown below.

Table 1
Molecular properties of IAPs and ABPs.

	IAPs	ABPs
Chemical composition		
Extraction yields (%)	4.49 ± 0.03[b]	10.33 ± 0.02[a]
Total polysaccharide (%)	58.84 ± 0.81[b]	90.79 ± 0.71[a]
Total Proteins (%)	6.78 ± 0.52[a]	1.67 ± 0.22[b]
Total Uronic acids (%)	3.33 ± 5.75[b]	10.38 ± 1.13[a]
Reducing sugar (%)	0.04 ± 0.01[b]	0.13 ± 0.01[a]
Mw (Da)		
Fraction 1 × 10^6	1.95 ± 0.18	5.40 ± 0.09
Relative peak areas (%)	24.71	95.77
Fraction 2 × 10^4 3.22 ± 0.13	3.22 ± 0.13	—
Relative peak areas (%)	52.73	—
Fraction 3 × 10^3	1.16 ± 0.03	1.88 ± 0.21
Relative peak areas (%)	16.85	4.23
Fraction 4 × 10^2	2.81 ± 0.36	—
Relative peak areas (%)	5.70	—
Monosaccharide composition (Relative%)		
Galactose	22.16	1.58
Glucose	53.34	40.6
Mannose	15.76	24.88
Xylose	—	17.88
Galacturonic acid	1.57	—
Glucuronic acid	2	14.16

Values are expressed as mean ± SD (n = 3). Means within a row with different letters indicate significant differences ($P \leq 0.05$).

$$\text{Scavenging activity (\%)} = [(A_1\text{-}A_2)/A_0] \times 100 \quad (1)$$

where A_1 denotes the absorbance of sample with DPPH–methanol solution, A_2 represents the absorbance of sample with methanol, and A_0 refers to the absorbance of distilled water with DPPH–methanol solution.

Hydroxyl radical scavenging activity

The hydroxyl radical eliminating potential was assessed via a procedure described previously (Tang & Huang, 2018). Initially, varying concentration IAPs and ABPs (50 μL) were added into 6 mM ferrous sulfate aqueous solution (50 μL) and 6 mM salicylic acid–ethanol solution, and subsequently1% hydrogen peroxide (50 μL) was added to initiate the reaction. Following 30 min of interaction at room temperature, the 510 nm absorbance was assessed (Spectra maxM5, Molecular Devices, USA), where the positive control was Vc. The computational equation for hydroxyl radical scavenging potential was shown below.

$$\text{Scavenging activity (\%)} = [(A_0\text{-}A_1)/A_0] \times 100 \quad (2)$$

where A_0 and A_1 represent the absorbances of the solvent control and the test sample (or Vc), respectively.

Reducing power

The assessment of reducing power was accomplished for IAPs and ABPs following the previous procedure (Jing et al., 2015; Tan et al., 2015). Briefly, 200 μL of samples with different concentrations were mixed with 100 μL ml of pH 6.6 phosphate buffer (0.2 M) and 100 μL mL of 1% (w/v) potassium ferricyanide solution, and preserved for 20 min at 50 ℃. The reaction was terminated by adding 10% (w/v) trichloroacetic acid solution (100 μL). Distilled water (400 μL) and 0.1% (w/v) ferric chloride solution (0.1 mL) were added and stored at room temperature for 10 min, followed by determination of the 700 nm sample absorbance, where the positive control was BHT.

Statistical analysis

The experiments were all triplicated. The results were presented as means ± SD. Map was drawn with Origin 2018, statistical processing was performed via SPSS 22.0, and significance evaluation on differences between data was accomplished through ANOVA.

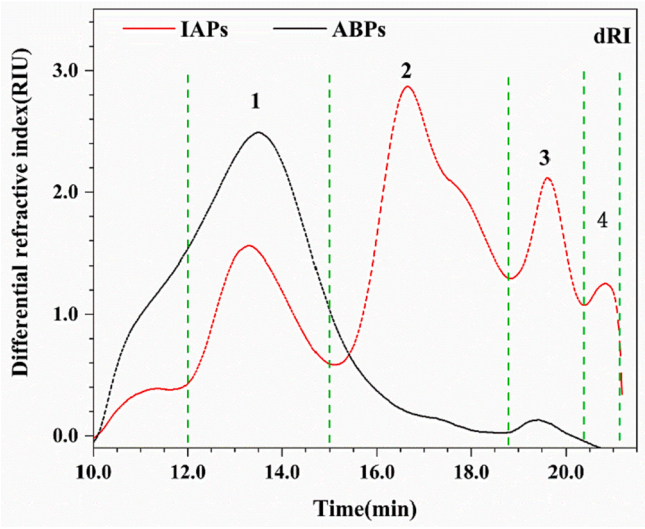

Fig. 1. Molecular weight distribution of IAPs and ABPs. IAPs, polysaccharides from mycelium of *Auricularia polytricha*; ABPs, polysaccharides from fruit body of *Auricularia polytricha*.

Results and discussion

Molecular properties

Chemical compositions

For the polysaccharide extracts from *Auriculariapolytricha* mycelium and fruit body, their chemical compositions and yields were summarized in Table 1. Comparison of the yields revealed ABPs > IAPs. There is almost no reducing sugar in both IAPs and ABPs. The total carbohydrate contents in IAPs and ABPs were 58.84 ± 0.81%, 90.79 ± 0.71% with significant difference, suggesting that IAPs and ABPs were the main components of *Auriculariapolytricha* mycelium and fruit body. In addition, proteins were found in both polysaccharides, which may indicate the presence of glycoprotein complex. The protein content of IAPs was higher (6.78 ± 0.52%), while that of ABPs was lower (1.67 ± 0.22%). There were more uronic acids in the ABPs than IAPs, and it was easier to form lactones.

Weight-average molecular weights and constituent monosaccharides of IAPs and ABPs

For natural polysaccharides, their bioactivities are associated with monosaccharide compositions and molar masses (Wu et al., 2018). The Fig. 1 showed the chromatograms of IAPs and ABPs. There were four polysaccharide components (components 1 to 4) detected in IAPs, while ABPs only existed in component 1 and component 3. For the fractions 1–4 in IAPs and ABPs, their particular molar masses, relative peak areas (%) and molar mass distributions are summarized in Table 1. In this study, the polysaccharide was extracted by ultrasonic extraction method. During the extraction process, high ultrasonic power can lower the molecular weight of polysaccharides, and the mycelium is more likely to be broken (Guo et al., 2019). IAPs exhibited broader range of molar mass distribution in comparison with ABPs. Nevertheless, the molar masses of IAPs were enriched between 3.22 × 10^4 Da (52.73%) and 1.95 × 10^6 Da (24.71%), accounting for 77.44%. Meanwhile, the molar masses of ABPs were localized in 5.4 × 10^6 Da, occupying 95.77% respectively.

In addition, the composition and concentrations of monosaccharides in mycelium also differ from those of fruit body. IAPs are made up of galactose (22.16%),glucose (53.34%), and mannose (15.76%), while ABPs are made up of galactose (1.58%), glucose (40.6%), mannose

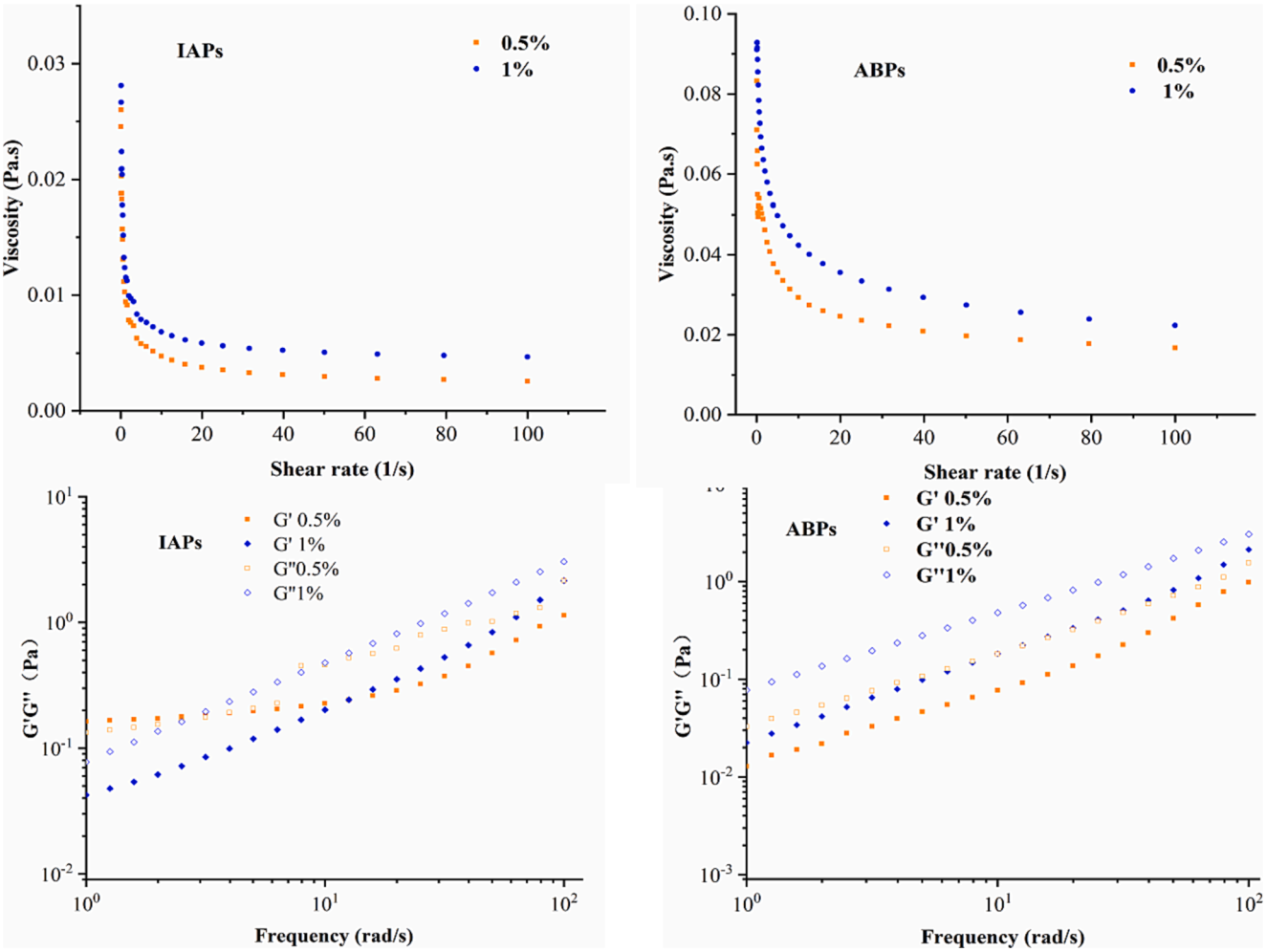

Fig. 2. Dependence of apparent viscosity on the shear rate and plots of storage modulus G′ and loss modulus G″ against frequency for IAPs and ABPs.

(24.88%), and xylose (17.88%), which are basically the same as a previous study (Chen et al., 2018). The glucuronic acid content varied significantly in the component composition of IAPs and ABPs, conforming to the conclusion that FT-IR spectroscopy analysis of the C═O telescopic vibration of the absorbent band esterified group at 1732 cm^{-1}. For IAPs, gene expression in the strain may result in the differences in polysaccharide structure (Liu, Zhu, Liu, & Sun, 2019).

Rheological properties of IAPs and ABPs

Polysaccharides have excellent functional traits, including foaming, emulsifying, thickening and gelling, which have long been examined and explored, and have also been used as gelatinous agents, thickeners and emulsifiers in industry (Gao et al., 2015;Wang, Zhang, Xiao, Huang, Li, & Fu, 2018). At present, there are numerous studies on the biological activities of *Auricularia polytricha* polysaccharides. Few of them involved the information concerning rheological behavior. Therefore, it is essential to study the apparent viscosity of IAPs and ABPs. The Fig. 2 shows how the shear rate influences the apparent viscosity of varying concentrations of ABPs and IAPs solutions under 25 ℃. Dependence of the two solutions' apparent viscosity on the concentration is noted, which is similar with Polysaccharide (Nie et al., 2019) in okra and pectin (Wang et al., 2016) in grapefruit peel. The viscosity elevation is associated probably with the fact that single molecules start overlapping to intensify the intermolecular connections formation when the polysaccharide concentration is high, and thus the polymer chain arrangement and stretching are limited and the apparent viscosity is intensified (Bae, Oh, Lee, Yoo, & Lee, 2008). The apparent viscosity decreases with the increase at stable shear conditions. In the range of low shear rate (0–50 s^{-1}), the shear-thinning performance of ABPs and IAPs solutions is non-Newtonian, while at high shear rates (50–100 s^{-1}), the polysaccharides show a flow behavior similar to Newton. It has been demonstrated that the shear-thinning performance of polysaccharides is associated probably with the molecular chains untangling in solution (Xu et al., 2019). In addition, the apparent viscosity of ABPs is stronger than that of IAPs, which may be linked to the carbohydrate concentration and molar mass. If the purity of IAPs can be further improved, ABPs can be replaced. Nevertheless, IAPs have excellent gel properties and are expected to be further developed as a food thickening agent

As a viscoelastic material, polysaccharides display both solid and liquid properties, which are dynamically measurable (Bao, Zhou, You, Wu, Wang, & Cui, 2018).The frequency sweep experiments is conducted under a 15 % constant strain, which is within the linear adhesive elastic region. As shown in the figure, the storage modulus (G') and loss modulus (G'') of ABPs and IAPs solutions (0.5 and 1 %; w/v) are enhanced with the increase in oscillation frequency. In the range of test frequencies, the G' value of the polysaccharide solution at a concentration of 1.0% was higher than that at the concentration of 0.5 %.This growth trend may be caused by the increased complexity and quantity of connection points between polymer chains when concentrations are higher, as confirmed by the previous studies (Simas-Tosin et al., 2010). The loss modulus is always greater than the storage modulus, which is contrary to the research conclusion of *Auricularia polytricha* fruit body polysaccharide in ABPs solution. During preshearing process, shear disrupts the entangled network structure of the molecular chain in

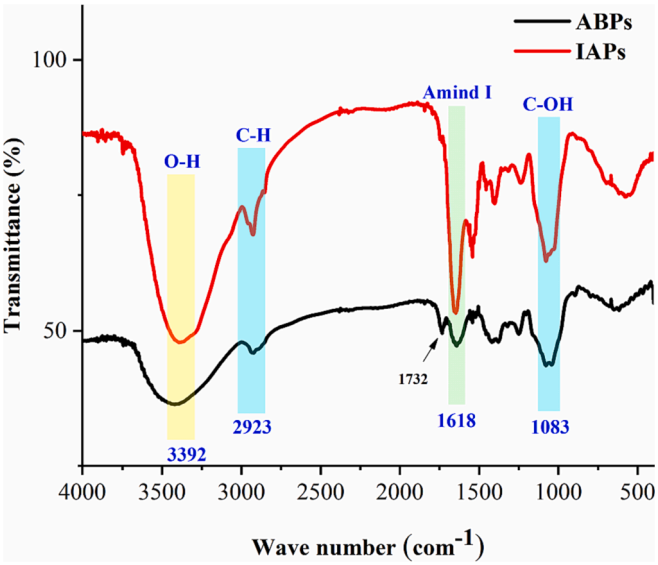

Fig. 3. FT-IR spectra of polysaccharide from mycelium and fruit body of *Auricularia polytricha*.

solution, arranging the molecules in an orderly manner. Then, the viscosity of the solution decreases, and G'' is greater than G', indicating that the ABPs solution has liquid-like properties. In IAPs solutions, 1% of the solution has always lost more than the stored module, similar to ABPs, indicating that the polymer also has liquid-like properties. At low frequencies, the storage modulus of polymer (0.5%) is greater than the loss modulus, besides, G' and G'' are changed, demonstrating the weak gel behavior of the organic polymer, with no crossover at high frequencies. This is related to the molecular weight, typically, the G'-G'' intersection preferably reflects the material's viscoelastic performance and defines the onset or approach the gel state, with the lower intersections indicating the greater elastic contribution. For different polysaccharides, the relationship between G'-G'' intersection and concentration has been debated.

FT-IR spectroscopy analysis of IAPs and ABPs

FT-IR is an analytical method for identifying the function groups in biological macromolecules, which, as a supplementary measure for structural analysis, enables the molecular structural and chemical bonds determination of polysaccharides (Zhao et al., 2019). As displayed in Fig. 3, polysaccharide feature absorption peaks generally appear between 4,000 and 400 cm^{-1} (Deng et al., 2020; Dou, Chen, & Fu, 2019). Near 3,394 cm^{-1}, there is a strong absorption band associated with O—H stretch vibration, which reveals the presence of hydrogen bonds between molecules. However, a weak peak around 2,925 cm^{-1} is ascribed to the tensiling vibration of C—H (Shi, Yin, Zhang, Huang, & Nie, 2019). ABPs shows stronger telescopic vibration than IAPs. Besides, the 1,732 cm^{-1} absorption peak of ABPs is assigned to the esterification group's C═O stretching vibration (Kpodo et al., 2017), which is almost absent in IAPs. The infrared spectra of ABPs differ significantly from that of IAPs. Combined with the findings discussed above, or with the composition of monosaccharides, where α-pyranose's characteristic absorption peak is located at 1,083 cm^{-1} (Deng et al., 2020), the signal near 1,651 cm^{-1} may be associated with N—H partial vibration in the amide group, consistent with the presence of small amounts of proteins (Chen, Huang, You, & Fu, 2017). Obviously, the main absorption peaks of the IAPs and ABPs are similar. Therefore, we can show that ABPs and IAP are not extremely different in organic groups, and IAPs may be capable of replacing ABPs.

Micromorphological characteristics analysis

The IAPs and ABPs scanning electroscope micro photograms are shown in Fig. 4. The microstructure and slight difference of polysaccharide surface can be observed by scanning electron microscope. The IAPs are sheet scattered and clustered, with rough surfaces and folds with pores at 1000× magnification, weakening with increasing

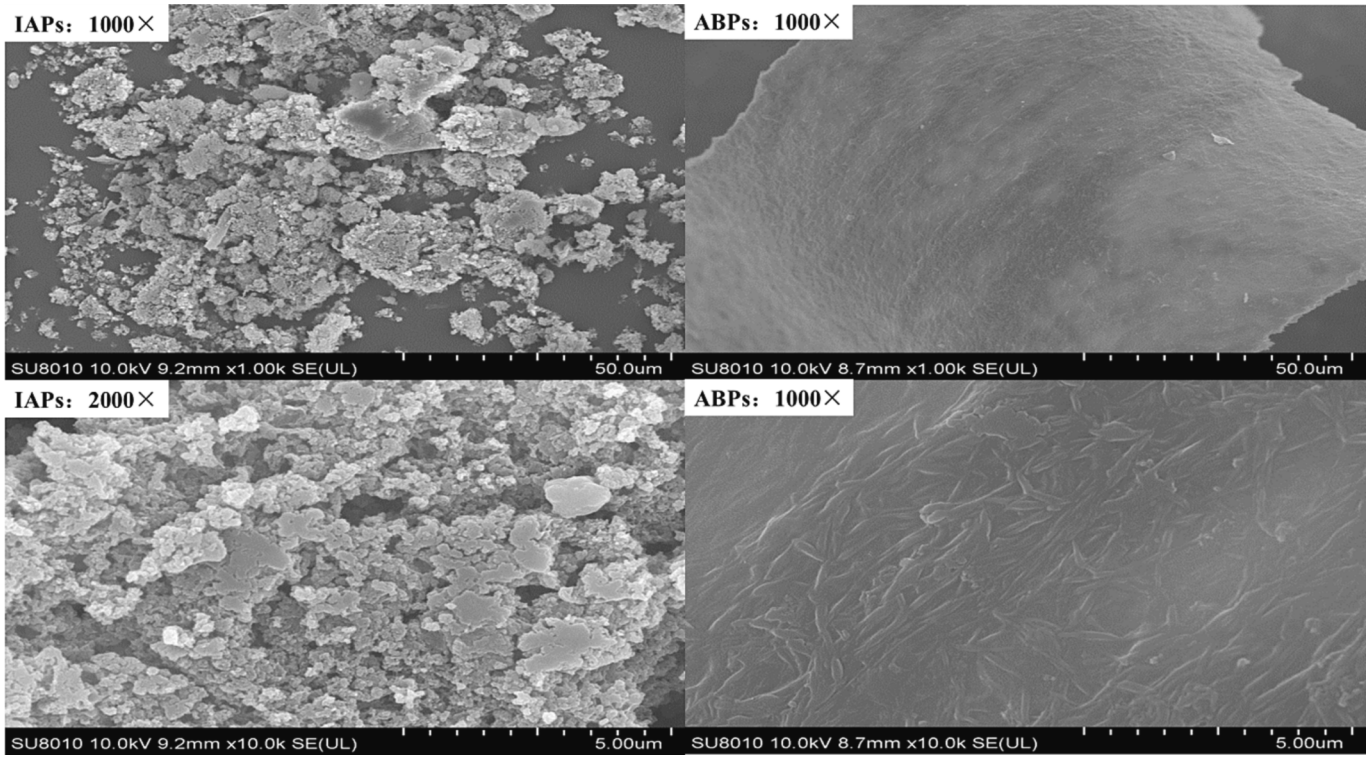

Fig. 4. SEM micrographs of IAPs (A); ABPs (B). IAPs, polysaccharides from mycelium of *Auricularia polytricha*; ABPs, polysaccharides from fruit body of *Auricularia polytricha*.

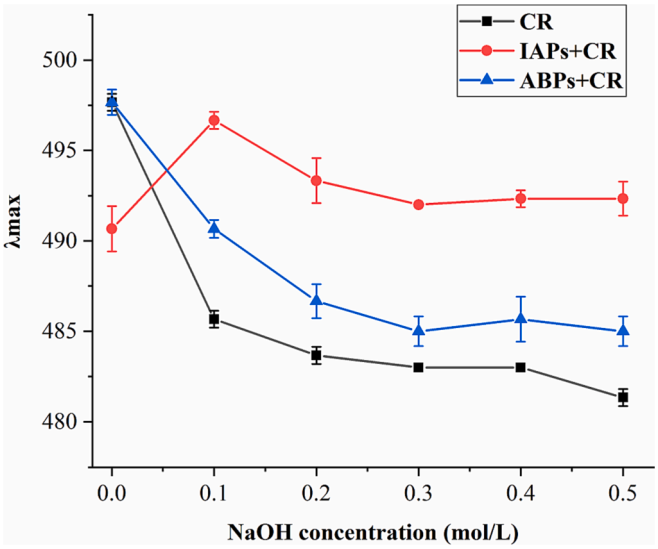

Fig. 5. Maximum absorption wavelength of Congo red-polysaccharide complex at various concentrations of NaOH solution. IAPs, polysaccharides from mycelium of *Auricularia polytricha*; ABPs, polysaccharides from fruit body of *Auricularia polytricha*. (For interpretation of the references to colour in this figure legend, the reader is referred to the web version of this article.)

magnification. Their surfaces are rather loose, rough and their structure is amorphous, suggesting the presence of interplays between the polysaccharides molecules(Wu et al., 2020). The ABPs structure is tightly knit and has a rough surface at 1000× magnification and a fine texture at 2000× magnification. identical extraction process is adopted for IAPs and ABPs, the surface microstructural disparity is probably attributable to their growth context. According to several researches, the monosaccharide composition was associated with the polysaccharide microstructure, particularly the uronic acid concentration (Ji, Hou, Yan, Shi, & Liu, 2020; Romdhane, Haddar, Ghazala, Jeddou, Helbert, & Ellouz-Chaabouni, 2017).

Congo red analysis

A crucial feature to maintain the biological activity of biopolymers is the triple helix conformation. A triple helix complex is formable by Congo red with polysaccharides in alkaline solution λ and the maximum has an obvious red shift (Shang, Chen, Li, Zhou, Wu, & Song, 2018).The maximum absorption wavelength of IAPs versus Congo red formed a redshift compared with Congo red, as shown in Fig. 5. Under the NaOH concentration of 0 M to 0.1 M, the UV absorption wavelength shifts to the long wave, indicating that the sample can form a complex with Congolese red, with a regular trisomy spiral image. When the concentration of NaOH continues to increase, the molecular hydrogen bond is destroyed, and the triple helix structure dissolves into a single strand, which becomes an irregular linear ball. This cannot be recombined with Congo red, and the maximum absorption wavelength decreases. In comparison with IAPs, the red shift of the maximum absorption wavelength of ABPs is obvious enough. Whether ABPs have a three strand helical conformation needs to be further investigated. The difference in the chain conformation of IAPs and ABPs in solution is linked probably to differences in their monosaccharide constitution, molar mass, and glycoside bonds.

Table 2
Thermal properties of polysaccharides.

	IAPs	ABPs
TGA analysis		
Bounding water (%)	3.77	3.69
Final weight (%)	25.00	26.77
DTG analysis (Decomposition rate and temperature)		
Peak-2	4.11 %/min	9.69 %/min
	285.2℃	275.9℃
Peak-3	3.38 %/min	—
	332.2℃	—

Thermal and XRD analysis

Thermal properties of IAPs and ABPs were examined through TG, DTG and DSC. For thermogravimetric analysis, the weight loss characteristics of IAPs and ABPs are different. It can be observed from TG and DTG curves that this may be related to the composition, aggregation state and water content of polysaccharides. Two phases were observed in IAPs and ABPs (Fig. 6AB). The first stage is attributable to the adsorption loss and bound water in biopolymers, which can be considered as dehydration peaks of sugar, with little difference between the amount of combined water (3.77% and 3.69 %).The second stage is mainly caused by chemical decomposition, during which the carbon skeleton of polysaccharides is greatly degraded (Chen, Zhao, Li, Hussain, Yan, & Wang, 2018; Derong Lin et al., 2018;Lin et al., 2019). Table 2 details the chemical decomposition, rate of decomposition and temperature information. At 275.9 ℃ (9.69 %/min), ABPs exhibited much higher decomposition rate than that of IAPs (4.11 %/min), and the final weight of IAPs (25.00%) and ABPs (26.77%), indicating that IAPs and ABPs exhibit good thermal stability and similar thermal stability. The DSC curve learns that there are peaks presenting at 478 ℃ and heat absorption at 88 ℃, resulting from oxidative decomposition and the latter from dehydration. The endothermic peak of ABPs appeared at 90 ℃, which was also caused by dehydration, and the exothermic peak appeared at 280 ℃ and 480 ℃. The former may be a weak exothermic peak due to rapid decomposition rate, while the latter is the decomposition of polysaccharides. It further suggests that IAPs and ABPs have similar thermal stability.

As an analytical technique for elucidating polysaccharide structures, XRD is often adopted for assessing the amorphous or crystal properties of polymers. According to Fig. 6C, IAPs and ABPs have a strong peak at

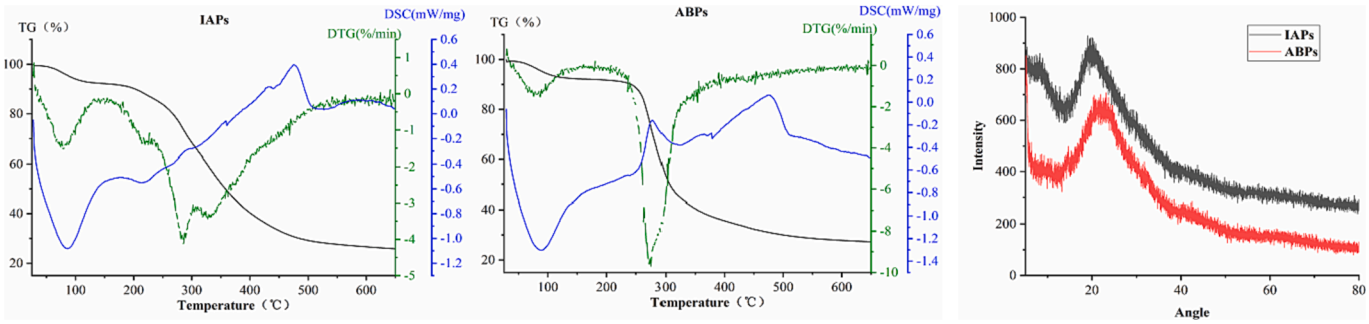

Fig. 6. Preliminary characterization of polysaccharides from mycelium and fruit body of *Auricularia polytricha*. (A), (B) Thermal gravimetric analysis and differential scanning calorimetry (TGA and DSC) thermograms. (C) X-ray diffraction (XRD).

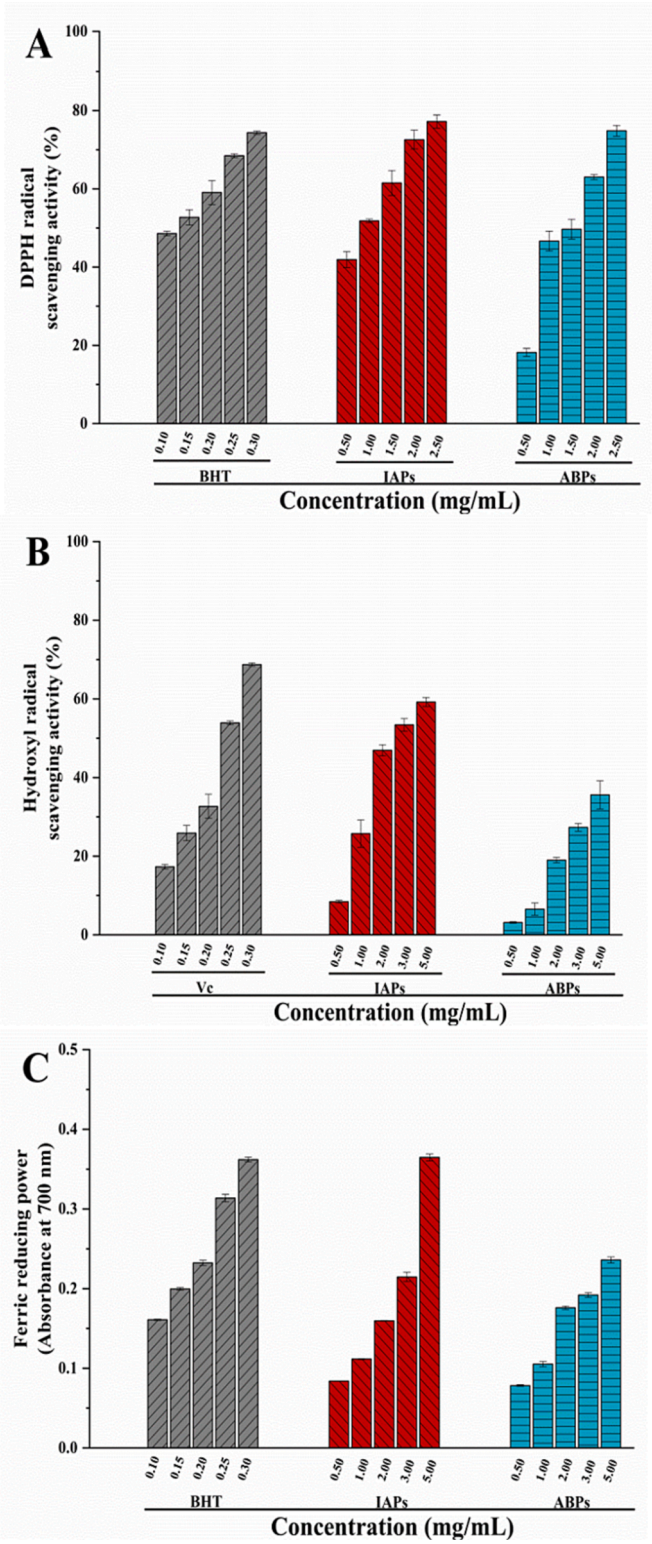

Fig. 7. DPPH radical cation scavenging capacity (A), Hydroxyl radical scavenging capacity(B), and Ferric reducing power (C) of IAPs and ABPs. IAPs, polysaccharides from mycelium of *Auricularia polytricha*; ABPs, polysaccharides from fruit body of *Auricularia polytricha*.

20θ. It is shown that the two polysaccharide crystal structures are similar. Both crystal structure and amorphous structure (Rozi et al., 2020) are consistent with the DSC finding.

Antioxidant activities of IAPs and ABPs

Fig. 7A, B, C showed the DPPH, Hydroxyl radical eliminating potentials and Ferric reducing power of the two polysaccharides. According to Fig. 7A, B and C, the DPPH, Hydroxyl radical eliminating potentials and Ferric reducing power were all dependent on the dose, and the findings are shown below.

DPPH radical scavenging activity

There has been extensive application of DPPH, a stable free radical, for assessing the free radical eliminating potential of natural compounds, which is accomplished by forming a stable DPPH molecule through hydrogen donation (Zhang et al., 2016). Fig. 7A depicts the ability of IAPs and ABPs to scavenge DPPH radicals compared with the ability of BHT used as a positive control to scavenge DPPH radicals over a 0.5–2.5 mg/mL concentration scope. When both the IAPs and ABPs concentrations are higher at 2.5 mg/mL, the DPPH radicals were eliminated by 77.19% and 74.84%, respectively. The DPPH scavenging assay showed that the mycelium polysaccharides IAPs (IC_{50} = 0.89 ± 0.22 mg/mL) was superior to ABPs (IC_{50} = 1.48 ± 0.63 mg/mL) concerning antioxidant activity at the assayed concentration. The results demonstrated that the DPPH scavenging effect varied among IAPs and ABPs. In our speculation, the differences of the two polysaccharides probably arise from their differences in carbohydrate content, monosaccharide composition, glycosidic links, uronic acid level, etc. (Ji et al., 2020).

Hydroxyl radical scavenging activity

As the most reactive ROS, Hydroxyl radical is capable of attacking DNA, proteins and other biomolecules (Sun et al., 2018). Fig. 7B describes the scavenging capacities of IAPs and ABPs against hydrogen peroxide, which are compared with that of ascorbic acid. At a higher concentration (5.0 mg/mL), IAPs (59.21%) exhibited better hydroxyl radical scavenging potential than ABPs (35.57%). At the assayed

Table 3
The content of reducing sugar (C_R) and Uronic acid at different time points of digestion in vitro.

Process	Time	Reducing sugar (mg/mL)	Uronic acid (μg/mL)	Reducing sugar (mg/mL)	Uronic acid (μg/mL)
		IAPs		ABPs	
Saliva digestion	15 min	0.108 ± 0.008^{a}	44.591 ± 0.12^{b}	0.207 ± 0.02^{a}	94.894 ± 0.63^{b}
	30 min	0.107 ± 0.011^{a}	47.773 ± 0.10^{a}	0.205 ± 0.18^{a}	98.379 ± 0.88^{a}
	1 h	0.109 ± 0.051^{a}	48.348 ± 0.53^{a}	0.206 ± 0.15^{a}	97.439 ± 0.71^{a}
Gastric digestion	30 min	0.196 ± 0.002^{a}	88.833 ± 0.13^{b}	0.196 ± 0.001^{a}	128.227 ± 0.23^{a}
	1 h	0.196 ± 0.005^{a}	90.500 ± 0.55^{b}	0.193 ± 0.002^{a}	124.894 ± 0.18^{b}
	2 h	0.202 ± 0.003^{a}	89.439 ± 0.23^{b}	0.205 ± 0.012^{a}	124.288 ± 0.22^{b}
	4 h	0.202 ± 0.009^{a}	93.848 ± 0.15^{ab}	0.199 ± 0.004^{a}	124.742 ± 0.16^{b}
	6 h	0.201 ± 0.013^{a}	95.458 ± 0.11^{a}	0.201 ± 0.005^{a}	123.379 ± 0.19^{b}
Intestinal digestion	30 min	0.311 ± 0.018^{a}	108.422 ± 0.39^{b}	0.253 ± 0.015^{a}	129.412 ± 0.29^{d}
	1 h	0.310 ± 0.037^{a}	105.352 ± 0.21^{c}	0.259 ± 0.043^{a}	138.326 ± 0.54^{c}
	2 h	0.319 ± 0.086^{a}	105.224 ± 0.42^{c}	0.261 ± 0.022^{a}	145.182 ± 0.59^{b}
	4 h	0.309 ± 0.012^{a}	109.461 ± 0.33^{b}	0.265 ± 0.045^{a}	156.522 ± 0.18^{a}
	6 h	0.313 ± 0.075^{a}	118.709 ± 0.81^{a}	0.261 ± 0.050^{a}	158.432 ± 0.36^{a}

Different letters showed significant differences among different times ($p < 0.05$) in the same digestive process.

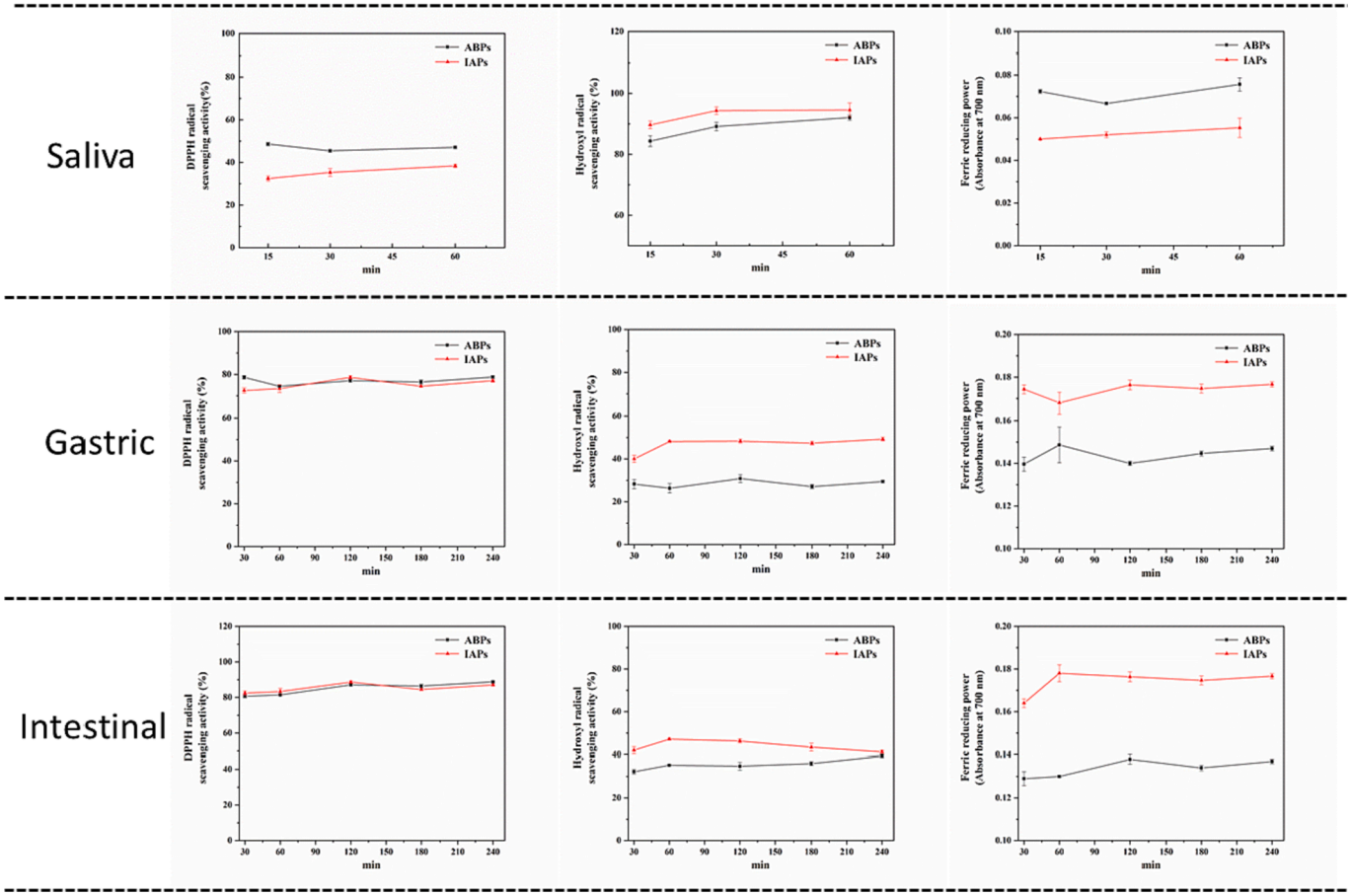

Fig. 8. Antioxidant activity measured by various methods of IAPs and ABPs after in vitro digestion (saliva, gastric and intestinal digests): DPPH radical scavenging activity assay; Hydroxyl radical scavenging assay; Ferric reducing power.

concentration, the IC_{50} of IAPs (3.37 ± 0.32 mg/mL) was higher compared to that of ABPs (6.56 ± 0.54 mg/mL). Hence, the polysaccharide-protein conjugate is conducive to IAPs' potential for radical elimination (Lu, Zhao, Sun, Yang, & Yang, 2013).

Reducing power

According to Fig. 7C, IAPs and ABPs led to the reduction of Fe^{3+}/$K_3Fe(CN)_6$ complex to Fe^{2+}ions; thus, monitoring of the Fe^{2+}ions was possible through the enhanced formation determination of Perl's Prussian blue at 700 nm (Lu et al., 2013). The dose-dependent effect was discernible over a 0.5–5.0 mg/mL concentration scope. At 5.0 mg/mL, reducing power was 0.36 for IAPs and 0.23 for ABPs. According to the present data, the two polysaccharides can be explored as potent antioxidants, despite their weaker oxidation resistance to the BHT reference. In general, IAPs were slightly higher than ABPs in antioxidant activity. The probable reason is that the molecular weight is low for IAPs and high for ABPs. Polysaccharides with low molecular weights have previously reported to possess strong antioxidant potential (Kelishomi et al., 2016; Yan, Wu, Qiao, Cai, & Ma, 2019).

Changes of reducing sugar contents and antioxidant activities of IAPs and ABPs during digestion

It was generally accepted that polysaccharides form aggregates easily in aqueous solution. Both the break of the polymer and the break of the covalent bond in the polymer chain contribute to the reduction of the molecular weight in polysaccharides. Nevertheless, the breakage of the glycosidic bonds leads to a quantity elevation of reducing ends. Content of α-amylase is high in the simulated saliva, which is the major human saliva enzyme capable of hydrolyzing α-(1 → 4)-glycosidic bond in carbohydrates including starch. Alterations in reducing sugar contents (CR) in the course of saliva–gastrointestinal digestion are detailed in Table 3 for IAPs and ABPs. Obviously, between 15 min and 1 h, there was no difference in the reducing sugar content during the simulated saliva digestion, suggesting that digestion of these two polysaccharides in simulated saliva was impossible. Actually, human saliva is incapable of digesting the majority of natural non-starch polysaccharides (Chen et al., 2018).There existed no significant change in CR value composition, implying that degradation of the two polysaccharides in the gastrointestinal digestive system was also impossible. Our result resembles that of a previous report (Chen et al., 2018). After 1 h of saliva digestion, DPPH of IAPs and ABPs was approximately 40.00% and 50.00%. DPPH maintained the stability at around 78.00% after digesting with gastric medium. Following digestion by small intestinal medium, DPPH increased by 10.00% (87.05%–88.78%).Such alteration resembles that of glucuronic acids (from approximately 44.591 μg/mL to 95.458 μg/mL and then to 118.709 μg/mL). This conclusion is consistent with the previous reports (Yuan et al., 2019).In terms of the DPPH radical scavenging activity outcomes, the antioxidant capacity exhibited a different trend from that of the hydroxyl radical eliminating capacity. The rate of hydroxyl radical clearance decreased from approximately 90% to 40% during the phase of saliva digestion to the phase of intestinal gestion. It is shown from Fig. 8 that the reduction force of IAPs and ABPs dissolved samples changed obviously as the time of dissipation increases. The reducing power-related absorption data demonstrated that the saliva, stomach fluid and intestinal digestive products of IAPs and ABPs have lower reduction force. This finding indicated pronounced effects of gastric and intestinal digestion on the

two polysaccharides' bioactivities, which probably arouse from the variations in their chemical traits and structure. In general, IAPs and ABPs were able to maintain some antioxidant activity during each phase of digestion.

Conclusion

The structure and simulated digestion of mycelium and fruit body polysaccharides (IAPs and ABPs) in vitro were studied. The spectral analysis results demonstrate that IAP and ABP are similar. In addition, both IAP and ABPs have good antioxidant activity, rheological properties and thermal properties. However, the two polysaccharides differ slightly in molar mass distribution and microphase structure. In addition, our results implied that the two polysaccharides are capable of passing through the digestive system (saliva, small intestine and stomach) without degradation to smoothly reach the large intestine. Hence, the physicochemical traits were explored in the current research, providing information about the invitro digestion of the two polysaccharides in the future. However, the inadequacies are that the mechanisms involved and the related activities or functions in vivo have not been investigated, which will be the focus of our following work. Although the polysaccharides were deproteinized in this study, the obtained polysaccharides were still crude, which possessed a lot of uncertainties. Moreover, the focuses of future research should be on the purification and elucidation of the biopolymers as well as on the clarification of association between structure and activity.

CRediT authorship contribution statement

Zhengbin Yang: Methodology, Formal analysis, Writing – original draft. **Yongde Zeng:** Resources. **Yuedan Hu:** Software. **Tingting Zhou:** Data curation. **Jiamin Li:** Visualization. **Lapin He:** Revising manuscript. **Wei Zhang:** Funding acquisition. **Xuefeng Zeng:** Revising manuscript. **Jin Fan:** Project administration.

Declaration of Competing Interest

The authors declare that they have no known competing financial interests or personal relationships that could have appeared to influence the work reported in this paper.

Data availability

Data will be made available on request.

Acknowledgments

This research was financially supported by the Key Project in Agricultural of Guizhou Province in [2019] 2337, 2379; [2022] key projects 013; Guizhou Science and Technology Program (Qian Ke He Jichu [2019] 1071).

Appendix A. Supplementary data

Supplementary data to this article can be found online at https://doi.org/10.1016/j.fochx.2023.100570.

References:

Bae, I. Y., Oh, I. K., Lee, S., Yoo, S. H., & Lee, H. G. (2008). Rheological characterization of levan polysaccharides from Microbacterium laevaniformans. *International Journal of Biological Macromolecules, 42*(1), 10–13. https://doi.org/10.1016/j.ijbiomac.2007.08.006

Bao, H., Zhou, R., You, S., Wu, S., Wang, Q., & Cui, S. W. (2018). Gelation mechanism of polysaccharides from Auricularia auricula-judae. *Food Hydrocolloids, 76*, 35–41. https://doi.org/10.1016/j.foodhyd.2017.07.023

Bradford, M. M. (1976). A rapid and sensitive method for the quantitation of microgram quantities of protein utilizing the principle of protein-dye binding. *Analytical Biochemistry, 72*(1–2), 248–254. https://doi.org/10.1016/0003-2697(76)90527-3

Chen, C., Huang, Q., You, L. J., & Fu, X. (2017). Chemical property and impacts of different polysaccharide fractions from Fructus Mori. on lipolysis with digestion model in vitro. *Carbohydrate Polymers, 178*, 360–367. https://doi.org/10.1016/j.carbpol.2017.09.015

Chen, G., Xie, M., Wan, P., Chen, D., Ye, H., Chen, L., … Liu, Z. (2018). Digestion under saliva, simulated gastric and small intestinal conditions and fermentation in vitro by human intestinal microbiota of polysaccharides from Fuzhuan brick tea. *Food Chemistry, 244*, 331–339. https://doi.org/10.1016/j.foodchem.2017.10.074

Chen, H., Zhao, C., Li, J., Hussain, S., Yan, S., & Wang, Q. (2018). Effects of extrusion on structural and physicochemical properties of soluble dietary fiber from nodes of lotus root. *Lwt, 93*, 204–211. https://doi.org/10.1016/j.lwt.2018.03.004

Chen, Y., & Xue, Y. (2018). Purification, chemical characterization and antioxidant activities of a novel polysaccharide from Auricularia polytricha. *International Journal of Biological Macromolecules, 120*(Pt A), 1087–1092. https://doi.org/10.1016/j.ijbiomac.2018.08.160

Deng, Y., Huang, L., Zhang, C., Xie, P., Cheng, J., Wang, X., & Liu, L. (2020). Novel polysaccharide from Chaenomeles speciosa seeds: Structural characterization, alpha-amylase and alpha-glucosidase inhibitory activity evaluation. *International Journal of Biological Macromolecules, 153*, 755–766. https://doi.org/10.1016/j.ijbiomac.2020.03.057

Ding, Y., Yan, Y., Peng, Y., Chen, D., Mi, J., Lu, L., … Cao, Y. (2019). In vitro digestion under simulated saliva, gastric and small intestinal conditions and fermentation by human gut microbiota of polysaccharides from the fruits of Lycium barbarum. *International Journal of Biological Macromolecules, 125*, 751–760. https://doi.org/10.1016/j.ijbiomac.2018.12.081

Dou, Z., Chen, C., & Fu, X. (2019). Digestive property and bioactivity of blackberry polysaccharides with different molecular weights. *Journal of Agricultural and Food Chemistry, 67*(45), 12428–12440. https://doi.org/10.1021/acs.jafc.9b03505

Dubois, M., Gilles, K. A., Hamilton, J. K., Rebers, P. t., & Smith, F. (1956). Colorimetric method for determination of sugars and related substances. *Analytical chemistry, 28*(3), 350-356. doi: 10.1021/ac60111a017.

Filisetti-Cozzi, T. M., & Carpita, N. C. (1991). Measurement of uronic acids without interference from neutral sugars. *Analytical biochemistry, 197*(1), 157–162. https://doi.org/10.1016/0003-2697(91)90372-Z

Fu, Y., Li, F., Ding, Y., Li, H. Y., Xiang, X. R., Ye, Q., … Wu, D. T. (2020). Polysaccharides from loquat (Eriobotrya japonica) leaves: Impacts of extraction methods on their physicochemical characteristics and biological activities. *International Journal of Biological Macromolecules, 146*, 508–517. https://doi.org/10.1016/j.ijbiomac.2019.12.273

Gao, J., Zhang, T., Jin, Z. Y., Xu, X. M., Wang, J. H., Zha, X. Q., & Chen, H. Q. (2015). Structural characterisation, physicochemical properties and antioxidant activity of polysaccharide from Lilium lancifolium Thunb. *Food Chemistry, 169*, 430–438. https://doi.org/10.1016/j.foodchem.2014.08.016

Guo, H., Yuan, Q., Fu, Y., Liu, W., Su, Y. H., Liu, H., … Wu, D. T. (2019). Extraction optimization and effects of extraction methods on the chemical structures and antioxidant activities of polysaccharides from snow chrysanthemum (Coreopsis Tinctoria). *Polymers (Basel), 11*(2). https://doi.org/10.3390/polym11020215

Ji, X., Hou, C., Yan, Y., Shi, M., & Liu, Y. (2020). Comparison of structural characterization and antioxidant activity of polysaccharides from jujube (Ziziphus jujuba Mill.) fruit. *International Journal of Biological Macromolecules, 149*, 1008–1018. https://doi.org/10.1016/j.ijbiomac.2020.02.018

Jing, Y., Zhu, J., Liu, T., Bi, S., Hu, X., Chen, Z., … Yu, R. (2015). Structural characterization and biological activities of a novel polysaccharide from cultured Cordyceps militaris and its sulfated derivative. *Journal of Agricultural and Food Chemistry, 63*(13), 3464–3471. https://doi.org/10.1021/jf505915t

Kelishomi, Z. H., Goliaei, B., Mahdavi, H., Nikoofar, A., Rahimi, M., Moosavi-Movahedi, A. A., … Bigdeli, B. (2016). Antioxidant activity of low molecular weight alginate produced by thermal treatment. *Food Chemistry, 196*, 897–902. https://doi.org/10.1016/j.foodchem.2015.09.091

Kpodo, F. M., Agbenorhevi, J. K., Alba, K., Bingham, R. J., Oduro, I. N., Morris, G. A., & Kontogiorgos, V. (2017). Pectin isolation and characterization from six okra genotypes. *Food Hydrocolloids, 72*, 323–330. https://doi.org/10.1016/j.foodhyd.2017.06.014

Lei, J., & Yang, D. (1990). The heavy metal content of edible fungi and the research of edible fungus heavy metal enrichment. *Chinese Edible Fungus, 9*, 14–17.

Lin, D., Huang, Y., Liu, Y., Luo, T., Xing, B., Yang, Y., … Qin, W. (2018). Physico-mechanical and structural characteristics of starch/polyvinyl alcohol/nano-titania photocatalytic antimicrobial composite films. *Lwt, 96*, 704–712. https://doi.org/10.1016/j.lwt.2018.06.001

Lin, D., Zhou, W., He, Q., Xing, B., Wu, Z., Chen, H., … Qin, W. (2019). Study on preparation and physicochemical properties of hydroxypropylated starch with different degree of substitution under microwave assistance. *International Journal of Biological Macromolecules, 125*, 290–299. https://doi.org/10.1016/j.ijbiomac.2018.12.031

Liu, X. C., Zhu, Z. Y., Liu, Y. L., & Sun, H. Q. (2019). Comparisons of the anti-tumor activity of polysaccharides from fermented mycelia and cultivated fruiting bodies of Cordyceps militaris in vitro. *International Journal of Biological Macromolecules, 130*, 307–314. https://doi.org/10.1016/j.ijbiomac.2019.02.155

Lu, X., Zhao, Y., Sun, Y., Yang, S., & Yang, X. (2013). Characterisation of polysaccharides from green tea of Huangshan Maofeng with antioxidant and hepatoprotective effects. *Food Chemistry, 141*(4), 3415–3423. https://doi.org/10.1016/j.foodchem.2013.06.058

Ma, L., Chen, H., Zhu, W., & Wang, Z. (2013). Effect of different drying methods on physicochemical properties and antioxidant activities of polysaccharides extracted from mushroom Inonotus obliquus. *Food Research International, 50*(2), 633–640. https://doi.org/10.1016/j.foodres.2011.05.005

Miller, G. L. (1959). Use of dinitrosalicylic acid reagent for determination of reducing sugar. *Analytical chemistry, 31*(3), 426–428. https://doi.org/10.1021/ac60147a030

Nie, X. R., Li, H. Y., Du, G., Lin, S., Hu, R., Li, H. Y., … Qin, W. (2019). Structural characteristics, rheological properties, and biological activities of polysaccharides from different cultivars of okra (Abelmoschus esculentus) collected in China. *International Journal of Biological Macromolecules, 139*, 459–467. https://doi.org/10.1016/j.ijbiomac.2019.08.016

Romdhane, M. B., Haddar, A., Ghazala, I., Jeddou, K. B., Helbert, C. B., & Ellouz-Chaabouni, S. (2017). Optimization of polysaccharides extraction from watermelon rinds: Structure, functional and biological activities. *Food Chemistry, 216*, 355–364. https://doi.org/10.1016/j.foodchem.2016.08.056

Rozi, P., Abuduwaili, A., Ma, S., Bao, X., Xu, H., Zhu, J., … Yili, A. (2020). Isolations, characterizations and bioactivities of polysaccharides from the seeds of three species Glycyrrhiza. *International Journal of Biological Macromolecules, 145*, 364–371. https://doi.org/10.1016/j.ijbiomac.2019.12.107

Sangphech, N., Sillapachaiyaporn, C., Nilkhet, S., & Chuchawankul, S. (2021). Auricularia polytricha ethanol crude extract from sequential maceration induces lipid accumulation and inflammatory suppression in RAW264. 7 macrophages. *Food & Function, 12*(21), 10563–10570. https://doi.org/10.1039/D0FO02574G

Shang, H., Chen, S., Li, R., Zhou, H., Wu, H., & Song, H. (2018). Influences of extraction methods on physicochemical characteristics and activities of Astragalus cicer L. polysaccharides. *Process Biochemistry, 73*, 220–227. https://doi.org/10.1016/j.procbio.2018.07.016

Sheu, F., Chien, P.-J., Chien, A.-L., Chen, Y.-F., & Chin, K.-L. (2004). Isolation and characterization of an immunomodulatory protein (APP) from the Jew's Ear mushroom Auricularia polytricha. *Food chemistry, 87*(4), 593–600. https://doi.org/10.1016/j.foodchem.2004.01.015

Shi, X.-D., Yin, J.-Y., Zhang, L.-J., Huang, X.-J., & Nie, S.-P. (2019). Studies on O-acetyl-glucomannans from Amorphophallus species: Comparison of physicochemical properties and primary structures. *Food Hydrocolloids, 89*, 503–511. https://doi.org/10.1016/j.foodhyd.2018.11.013

Simas-Tosin, F. F., Barraza, R. R., Petkowicz, C. L. O., Silveira, J. L. M., Sassaki, G. L., Santos, E. M. R., … Iacomini, M. (2010). Rheological and structural characteristics of peach tree gum exudate. *Food Hydrocolloids, 24*(5), 486–493. https://doi.org/10.1016/j.foodhyd.2009.12.010

Sun, L., Wang, L., & Zhou, Y. (2012). Immunomodulation and antitumor activities of different-molecular-weight polysaccharides from Porphyridium cruentum. *Carbohydrate Polymers, 87*(2), 1206–1210. https://doi.org/10.1016/j.carbpol.2011.08.097

Sun, Y., Hou, S., Song, S., Zhang, B., Ai, C., Chen, X., & Liu, N. (2018). Impact of acidic, water and alkaline extraction on structural features, antioxidant activities of Laminaria japonica polysaccharides. *International Journal of Biological Macromolecules, 112*, 985–995. https://doi.org/10.1016/j.ijbiomac.2018.02.066

Tan, L. H., Zhang, D., Yu, B., Zhao, S. P., Wang, J. W., Yao, L., & Cao, W. G. (2015). Antioxidant activity and optimization of extraction of polysaccharide from the roots of Dipsacus asperoides. *International Journal of Biological Macromolecules, 81*, 332–339. https://doi.org/10.1016/j.ijbiomac.2015.08.022

Tang, Q., & Huang, G. (2018). Preparation and antioxidant activities of cuaurbit polysaccharide. *International Journal of Biological Macromolecules, 117*, 362–365. https://doi.org/10.1016/j.ijbiomac.2018.05.213

Tang, Z., Fan, J., Zhang, Z., Zhang, W., Yang, J., Liu, L., … Zeng, X. (2021). Insights into the structural characteristics and in vitro starch digestibility on steamed rice bread as affected by the addition of okara. *Food Hydrocolloids, 113*. https://doi.org/10.1016/j.foodhyd.2020.106533

Tenore, G. C., Campiglia, P., Giannetti, D., & Novellino, E. (2015). Simulated gastrointestinal digestion, intestinal permeation and plasma protein interaction of white, green, and black tea polyphenols. *Food Chemistry, 169*, 320–326. https://doi.org/10.1016/j.foodchem.2014.08.006

Wang, L., Zhang, B., Xiao, J., Huang, Q., Li, C., & Fu, X. (2018). Physicochemical, functional, and biological properties of water-soluble polysaccharides from Rosa roxburghii Tratt fruit. *Food Chemistry, 249*, 127–135. https://doi.org/10.1016/j.foodchem.2018.01.011

Wang, W., Ma, X., Jiang, P., Hu, L., Zhi, Z., Chen, J., … Liu, D. (2016). Characterization of pectin from grapefruit peel: A comparison of ultrasound-assisted and conventional heating extractions. *Food Hydrocolloids, 61*, 730–739. https://doi.org/10.1016/j.foodhyd.2016.06.019

Wu, D.-T., Guo, H., Lin, S., Lam, S.-C., Zhao, L., Lin, D.-R., & Qin, W. (2018). Review of the structural characterization, quality evaluation, and industrial application of Lycium barbarum polysaccharides. *Trends in Food Science & Technology, 79*, 171–183. https://doi.org/10.1016/j.tifs.2018.07.016

Wu, L., Sun, H., Hao, Y., Zheng, X., Song, Q., Dai, S., & Zhu, Z. (2020). Chemical structure and inhibition on alpha-glucosidase of the polysaccharides from Cordyceps militaris with different developmental stages. *International Journal of Biological Macromolecules, 148*, 722–736. https://doi.org/10.1016/j.ijbiomac.2020.01.178

Xiao, L., Sun, S., Li, K., Lei, Z., Shimizu, K., Zhang, Z., & Adachi, Y. (2020). Effects of nanobubble water supplementation on biomass accumulation during mycelium cultivation of Cordyceps militaris and the antioxidant activities of extracted polysaccharides. *Bioresource Technology Reports, 12*. https://doi.org/10.1016/j.biteb.2020.100600

Xu, Y., Liu, N., Fu, X., Wang, L., Yang, Y., Ren, Y., … Wang, L. (2019). Structural characteristics, biological, rheological and thermal properties of the polysaccharide and the degraded polysaccharide from raspberry fruits. *International Journal of Biological Macromolecules, 132*, 109–118. https://doi.org/10.1016/j.ijbiomac.2019.03.180

Yan, J. K., Wu, L. X., Qiao, Z. R., Cai, W. D., & Ma, H. (2019). Effect of different drying methods on the product quality and bioactive polysaccharides of bitter gourd (Momordica charantia L.) slices. *Food Chemistry, 271*, 588–596. https://doi.org/10.1016/j.foodchem.2018.08.012

Yang, Z., Hu, Y., Wu, J., Liu, J., Zhang, F., Ao, H., … Zeng, X. (2022). High-efficiency production of Auricularia polytricha polysaccharides through yellow slurry water fermentation and its structure and antioxidant properties. *Frontiers in Microbiology, 13*, Article 811275. https://doi.org/10.3389/fmicb.2022.811275

Yu, J., Sun, R., Zhao, Z., & Wang, Y. (2014). Auricularia polytricha polysaccharides induce cell cycle arrest and apoptosis in human lung cancer A549 cells. *International Journal of Biological Macromolecules, 68*, 67–71. https://doi.org/10.1016/j.ijbiomac.2014.04.018

Yuan, Y., Li, C., Zheng, Q., Wu, J., Zhu, K., Shen, X., & Cao, J. (2019). Effect of simulated gastrointestinal digestion in vitro on the antioxidant activity, molecular weight and microstructure of polysaccharides from a tropical sea cucumber (Holothuria leucospilota). *Food Hydrocolloids, 89*, 735–741. https://doi.org/10.1016/j.foodhyd.2018.11.040

Zhang, Z., Ding, X., Xu, Z., Wu, X., Yang, C., Hao, J., & Chen, Y. (2020). Optimization of ultrasonic/microwave assisted extraction (UMAE) and rheological properties of polysaccharides from Auricularia polytricha. *American Journal of Biochemistry and Biotechnology, 16*(1), 112–124. https://doi.org/10.3844/ajbbsp.2020.112.124

Zhang, Z., Kong, F., Ni, H., Mo, Z., Wan, J. B., Hua, D., & Yan, C. (2016). Structural characterization, alpha-glucosidase inhibitory and DPPH scavenging activities of polysaccharides from guava. *Carbohydrate Polymers, 144*, 106–114. https://doi.org/10.1016/j.carbpol.2016.02.030

Zhao, H., Li, H., Lai, Q., Yang, Q., Dong, Y., Liu, X., … Jia, L. (2019). Antioxidant and hepatoprotective activities of modified polysaccharides from Coprinus comatus in mice with alcohol-induced liver injury. *International Journal of Biological Macromolecules, 127*, 476–485. https://doi.org/10.1016/j.ijbiomac.2019.01.067

Zhao, S., Rong, C., Liu, Y., Xu, F., Wang, S., Duan, C., … Wu, X. (2015). Extraction of a soluble polysaccharide from Auricularia polytricha and evaluation of its anti-hypercholesterolemic effect in rats. *Carbohydrate Polymers, 122*, 39–45. https://doi.org/10.1016/j.carbpol.2014.12.041

Zhao, Y., Hu, W., Zhang, H., Ding, C., Huang, Y., Liao, J., … Yuan, M. (2019). Antioxidant and immunomodulatory activities of polysaccharides from the rhizome of Dryopteris crassirhizoma Nakai. *International Journal of Biological Macromolecules, 130*, 238–244. https://doi.org/10.1016/j.ijbiomac.2019.02.119

Zhou, W., Yan, Y., Mi, J., Zhang, H., Lu, L., Luo, Q., … Cao, Y. (2018). Simulated digestion and fermentation in vitro by human gut microbiota of polysaccharides from bee collected pollen of Chinese wolfberry. *Journal of Agricultural and Food Chemistry, 66*(4), 898–907. https://doi.org/10.1021/acs.jafc.7b05546